

Mechanistic Studies of Hangman Salophen-Mediated Activation of O–O Bonds

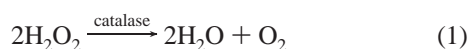
Shih-Yuan Liu,[†] Jake D. Soper,[†] Jenny Y. Yang,[†] Elena V. Rybak-Akimova,[‡] and Daniel G. Nocera^{*†}

Department of Chemistry, 6-335, Massachusetts Institute of Technology, 77 Massachusetts Avenue, Cambridge, Massachusetts 02139-4307, and Department of Chemistry, Tufts University, 62 Talbot Avenue, Medford, Massachusetts 02155

Received February 6, 2006

Stopped-flow kinetic studies of a HSX–Mn–SalophOMe (**1**) catalyst provide spectroscopic evidence for the direct generation of a manganese(V) oxo salophen from a manganese(III) perbenzoate. The O–O bond heterolysis reaction that produces the oxo is not facilitated by intramolecular proton transfer from the acid hanging group of the HSX platform. Instead, the hanging group stabilizes the catalyst against oxidative degradation and, consistent with recent predictions of theory, is geometrically matched to promote the end-on coordination of a H₂O₂ substrate prior to its oxidation at the manganese(V) oxo center.

Proton-coupled electron transfer (PCET) is a fundamental process that is involved in a number of important small-molecule bond-making and bond-breaking catalysis in nature.^{1–3} One such reaction is the disproportionation of H₂O₂, which is accomplished by catalase enzymes⁴ to remove cytotoxic H₂O₂ according to the following equation:



The key step of this reaction involves the activation of the O–O bond of H₂O₂ by heterolysis to produce the high-valent metal oxo species. Mutagenesis studies of O–O-activating enzymes establish that acid–base amino acids on the distal side of the redox cofactor perturb activity by affecting O–O bond heterolysis.⁵ In contrast, theoretical analysis^{6,7} predicts

that the O–O bond heterolysis in catalase model systems is facile and consequently requires little assistance from distal acid–base functionalities.

We have successfully captured the active site of catalase enzymes by designing synthetic Hangman constructs that precisely position an acid–base functionality from a xanthen spacer over the face of porphyrin^{8–10} and salophen¹¹ redox cofactors. In these systems, the distal function of the enzymes is faithfully modeled by the acid–base hanging group,^{1,8,10} thus allowing us to compare the chemistry of model catalase systems to their biological counterparts. In this Communication, we provide direct spectroscopic evidence for the production of manganese(V) oxo upon O–O bond heterolysis at the Hangman salophen platform. This intermediate is often cited as the active catalyst in model¹² and enzymatic systems, but its characterization heretofore has remained elusive.^{13,14} In accordance with theoretical predictions of the salen catalase models,^{6,7} the stopped-flow results show that the rate for production of the high-valent oxo at the salen platform is independent of the distal acid–base functional group.

Stopped-flow kinetic experiments on a HSX–Mn^{III}–SalophOMe (**1**) catalyst (Chart 1) were performed using *m*-CPBA as the O atom source. *m*-CPBA allows us to arrest the catalase cycle and detect intermediates at the Hangman salophen platform. The initial stage of the reaction after the addition of *m*-CPBA to **1** is characterized by small changes in the stopped-flow UV–vis spectrum (shown in Figure S3 of the Supporting Information), suggesting a simple ligand substitution by the perbenzoate at the Mn^{III} center. This substitution reaction was modeled by the addition of benzoic

* To whom correspondence should be addressed. E-mail: nocera@mit.edu.

[†] Massachusetts Institute of Technology.

[‡] Tufts University.

- (1) Chang, C. J.; Chang, M. C. Y.; Damrauer, N. H.; Nocera, D. G. *Biophys. Biochim. Acta* **2004**, *1655*, 13–28.
- (2) Stubbe, J.; Nocera, D. G.; Yee, C. S.; Chang, M. C. Y. *Chem. Rev.* **2003**, *103*, 2167–2202.
- (3) Cukier, R. I.; Nocera, D. G. *Annu. Rev. Phys. Chem.* **1998**, *49*, 337–369.
- (4) Nicholls, P.; Fita, I.; Loewen, P. C. *Adv. Inorg. Chem.* **2001**, *51*, 51–106.
- (5) Ozaki, S.-I.; Roach, M. P.; Matsui, T.; Watanabe, Y. *Acc. Chem. Res.* **2001**, *34*, 818–825.
- (6) Abashkin, Y. G.; Burt, S. K. *Inorg. Chem.* **2005**, *44*, 1425–1432.
- (7) Abashkin, Y. G.; Burt, S. K. *J. Phys. Chem. B* **2004**, *108*, 2708–2711.

- (8) Yeh, C.-Y.; Chang, C. J.; Nocera, D. G. *J. Am. Chem. Soc.* **2001**, *123*, 1513–1514.
- (9) Chng, L. L.; Chang, C. J.; Nocera, D. G. *Org. Lett.* **2003**, *5*, 2421–2424.
- (10) Chang, C. J.; Chng, L. L.; Nocera, D. G. *J. Am. Chem. Soc.* **2003**, *125*, 1866–1876.
- (11) Liu, S.-Y.; Nocera, D. G. *J. Am. Chem. Soc.* **2005**, *127*, 5278–5279.
- (12) McGarrigle, E. M.; Gilheany, D. G. *Chem. Rev.* **2005**, *105*, 1563–1602.
- (13) Sabater, M. J.; Alvaro, M.; Garcia, H.; Palomares, E.; Scaiano, J. C. *J. Am. Chem. Soc.* **2001**, *123*, 7074–7080.
- (14) Srinivasan, K.; Michaud, P.; Kochi, J. K. *J. Am. Chem. Soc.* **1986**, *108*, 2309–2320.

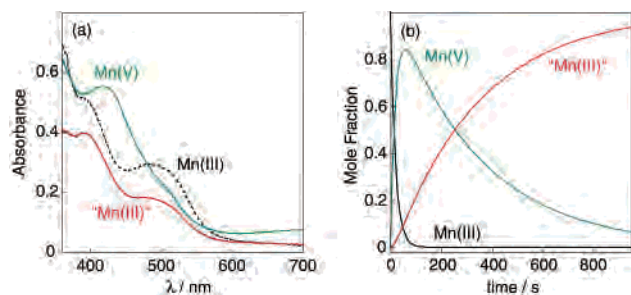
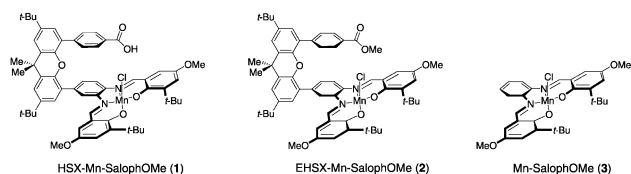


Figure 1. (a) Absorption spectra obtained from spectral global analysis of a stopped-flow reaction of 4.0×10^{-5} M **1** and 3.3×10^{-4} M *m*-CPBA in 1:1 MeOH/MeCN at -20 °C. Formation of manganese(V) oxo (green solid line) is immediately followed by a bleach, likely to a Mn^{III} decay product (red solid line) over 800 s. (b) Calculated concentrations of the colored species with respect to time by spectral global analysis.

Chart 1



acid to **1**. The benzoate substrate circumvents the possibility of O–O bond cleavage, therefore allowing the substitution reaction to be isolated. The small spectral shifts observed for perbenzoate substitution are captured with the benzoate model (Figure S3b of the Supporting Information). Global fitting of the transient spectra indicates that ligand substitution is complete in 3 s at -20 °C.

The appearance of the manganese(III) perbenzoate complex (Figure 1a, black dotted line) is immediately followed by a subsequent reaction that generates a species with the spectrum shown by the green line in Figure 1a. The spectrum does not depend on the nature of the oxidant; a similar spectrum is obtained with the same isosbestic points when *m*-CPBA is replaced by the two-electron oxidant, iodosylbenzene. These results lead us to assign the intermediate to the manganese(V) oxo salophen produced by heterolytic cleavage. Several observations support this assignment. First, the transient spectrum is reminiscent to that of structurally similar, crystallographically characterized manganese(V) oxo complexes of bis-amido bis-alkoxo redox platforms.¹⁵ Moreover, the spectral features in Figure 1a (green line) are similar in form to those of other (nonoxo) multiply bonded manganese(V) salophen ligand species. We have synthesized and isolated the corresponding nitrido complex Mn(N)–SalophOMe (see Supporting Information). The crystal structure of the compound (Figure S2 of the Supporting Information) is similar to that of other manganese(V) nitrido complexes featuring a formal Mn–N triple bond [$d(\text{Mn–N}) = 1.523(3)$ Å].¹⁶ The absorption spectrum of the Mn^V complex (Figure S1 of the Supporting Information) shows a pronounced absorption band at $\lambda_{\text{max}} = 459$ nm, similar to the 420-nm feature that dominates the absorption spectrum of

Table 1. Rates of Formation of Manganese(V) Oxo Intermediates and Their Decay for a Series of Mn–Salophen Complexes^a

$$\text{Mn(III)-(H)OOCAr} \xrightarrow{k_1} \text{Mn(V)-oxo} \xrightarrow{k_2} \text{Mn(III)}$$

entry	Mn complex	k_1 (s ⁻¹)	k_2 (s ⁻¹)
1	HSX–Mn–SalophOMe (1)	$2.3 \pm 0.6 \times 10^{-2}$	$3.6 \pm 0.3 \times 10^{-3}$
2	EHSX–Mn–SalophOMe (2)	$2.8 \pm 0.8 \times 10^{-2}$	$2.5 \pm 0.3 \times 10^{-3}$
3	Mn–SalophOMe (3)	$2.1 \pm 0.5 \times 10^{-2}$	$4.1 \pm 0.3 \times 10^{-3}$
4	HSX–Mn–SalophOMe (1) ^b	$2.9 \pm 0.6 \times 10^{-2}$	$5.5 \pm 0.5 \times 10^{-3}$

^a Rate constants determined with global analysis using a $A \rightarrow B \rightarrow C$ kinetic model. All reactions at -20 °C in 1:1 MeOH/MeCN with $[\text{Mn}^{\text{III}}] = 4.0 \times 10^{-5}$ M and $[\text{m-CPBA}] = 3.3 \times 10^{-4}$ M. ^b $[\text{m-CPBA}] = 13 \times 10^{-4}$ M.

Figure 1a (green line). Although the energies of the transitions are not congruent, the intensity and energy regime of the transition are consistent with the spectra of d^2 metal–ligand multiple bonds.

The electron-donating methoxy groups on the salophen platform of the manganese(V) oxo species impart sufficient stability¹⁷ such that it is observed as a stopped-flow transient. Notwithstanding, the reactive high-valent oxo intermediate eventually disappears 60–800 s after *m*-CPMA injection, as evidenced by the decrease of the absorption profile across the entire spectral range (360–700 nm). The final spectrum, shown by the red line in Figure 1a, strongly resembles the Mn^{III} starting material, though the product was not unequivocally identified.

The rate constants for the O–O bond heterolysis to produce the manganese(V) oxo salophen and its subsequent decay were obtained from global analysis of the full-spectral stopped-flow data (360–700 nm). The data were best fit to a consecutive unimolecular kinetic model in which the $A \rightarrow B$ phase represents the heterolytic O–O bond cleavage to furnish the manganese(V) oxo transient, and the $B \rightarrow C$ phase corresponds to the decay of the transient to the final Mn^{III} species. Figure 1b illustrates the calculated concentrations of each of the Mn species with respect to time according to this kinetic model, and Table 1 provides the rate constants for the kinetic model.

We note several features of the kinetic analysis: (1) Both the growth of the Mn^V transient spectrum and the decay of the Mn^{III} reactant are simultaneously fit well by a first-order exponential equation, indicating that heterolytic cleavage to generate manganese(V) oxo occurs without intermediates. This result is consistent with the heterolysis of O–O bonds of peroxides at iron(III) heme centers to form compound **I**.^{18–20} (2) The production of the manganese(V) oxo intermediate is independent of the presence of the hanging acid–base group (entry 1 vs 3 in Table 1) or intramolecular proton inventory (entry 1 vs 2 in Table 1). (3) The rate of the O–O bond heterolysis appears to be independent of the initial concentration of the *m*-CPBA oxidant (entry 1 vs 4 in Table

(15) McDonnell, F. M.; Fackler, N. L. P.; Stern, C.; O'Halloran, T. V. *J. Am. Chem. Soc.* **1994**, *116*, 7431–7432.

(16) Du Bois, J.; Hong, J.; Carreira, E. M.; Day, M. W. *J. Am. Chem. Soc.* **1996**, *118*, 915–916.

(17) Feichtinger, D.; Plattner, D. *Chem.–Eur. J.* **2001**, *7*, 591–599.

(18) Davydov, R.; Makris, T. M.; Kofman, V.; Werst, D. E.; Sligar, S. G.; Hoffman, B. M. *J. Am. Chem. Soc.* **2001**, *123*, 1403–1415.

(19) Ogliaro, F.; de Visser, S. P.; Cohen, S.; Sharma, P. K.; Shaik S. *J. Am. Chem. Soc.* **2002**, *124*, 2806–2817.

(20) Groves, J. T.; Watanabe, Y. *J. Am. Chem. Soc.* **1988**, *110*, 8443–8452.

Table 2. Turnover Number (TON) for the Catalytic Dismutation of H₂O₂ and Kinetic Stability of Methoxy-Substituted Manganese Salophen Complexes

Mn complex	yield of O ₂ /TON ^a	k _{obs} (s ⁻¹)
HSX-Mn-SalophOMe (1)	4500	2.9 × 10 ⁻⁴
EHSX-Mn-SalophOMe (2)	550	1.3 × 10 ⁻³
Mn-SalophOMe (3)	100 ^b	2.3 × 10 ⁻³

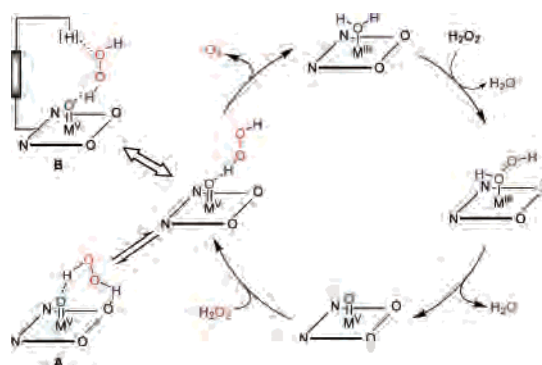
^a Yield of O₂ measured in TON after 1 h of reaction time. ^b In the presence of 1 equiv of benzoic acid.

1) though an increase in the *m*-CPBA concentration results in a slightly enhanced decay of the manganese(V) oxo intermediate (*k*₂ in entry 1 vs 4 in Table 1).

Whereas the hanging acid–base group is not manifested in O–O bond heterolysis, the data for catalytic dismutation of H₂O₂ indicate that it is crucial to catalytic turnover. As can be seen from Table 2, high turnover numbers can be achieved for the disproportionation of H₂O₂ at the Hangman platform **1**. On the other hand, low reactivity is observed when the carboxylic acid functionality is replaced by an ester or when a redox-only manganese salophen complex is used.

To address the role of the intramolecular proton inventory on enhancing the turnover number, we monitored **1** in the presence of H₂O₂ (30% aqueous solution in MeOH) in homogeneous solution conditions. The UV–vis absorption spectrum shows that the Mn^{III} starting material gradually decomposes over time. Kinetic experiments show that decomposition of **1** is first-order with respect to the Mn^{III} complex and H₂O₂ and zero-order with respect to H₂O. The decomposition of the ligand may suggest homolytic O–O bond cleavage to generate radical species as a minor competing mechanism. As shown by the rate constants in Table 2, the Hangman architecture improves the kinetic stability of the salophen catalyst against oxidative degradation by ~1 order of magnitude. This increased stability accounts for the higher turnover numbers listed in Table 2 for the Hangman salophen system.

Our mechanistic results concur with recent density functional theory predictions for the disproportionation of H₂O₂ by manganese-salen-derived catalysts.^{6,7} The calculated reaction pathway is illustrated in Scheme 1. Coordination of H₂O₂ to Mn^{III} is followed by heterolytic O–O bond cleavage to furnish a high-valent manganese(V) oxo intermediate. PCET activation of the O–O bond is accomplished by an intramolecular proton transfer of the H₂O₂ substrate without the need for an additional proton shuttle. The calculations establish that the end-on binding of H₂O₂ is the most productive approach for substrate oxidation by the manganese(V) oxo center. H bonding to the O atoms of the salen platform leads to temporary catalyst deactivation by forming kinetically stable intermediates, sending the reaction off-cycle (Scheme 1, **A**). The hanging acid–base group of the Hangman construct can keep the catalyst on cycle by promoting the

Scheme 1

end-on assembly of H₂O₂ via a H-bonding network (Scheme 1, **B**). The utility of the hanging group for the assembly of substrates in the second coordination sphere of redox platforms has been observed previously by us in the construction of a H₂O channel above the face of Hangman porphyrins.⁸ In promoting the end-on association of H₂O₂ in the Hangman pocket, the hanging group averts temporary catalyst deactivation arising from geometrically disadvantageous binding modes of H₂O₂.

In summary, stopped-flow kinetic studies of the reaction of **1** with *m*-CPBA give rise to spectra that are consistent with the initial rapid formation of a peracid-bound Mn^{III} species followed by direct generation of a high-valent manganese(V) oxo intermediate by O–O bond heterolysis. The use of *m*-CPBA as opposed to H₂O₂ as the peroxide substrate allows the reaction to be arrested after O–O bond heterolysis, thereby allowing the manganese(V) oxo to be built up and detected with facility. The stopped-flow kinetic results for the production of the manganese(V) oxo are in accordance with recent theoretical predictions that a distal group on a salen/salophen model is not needed for O–O bond cleavage. The role of the hanging group is to stabilize the catalyst against oxidative degradation and potentially to promote the end-on assembly of H₂O₂ above the redox platform for its subsequent oxidation by the manganese(V) oxo. Current studies are focused on directly probing the effect of the distal hanging group on the substrate assembly within the Hangman cleft of the HSX-Mn-SalophOMe catalysts.

Acknowledgment. This work was supported by funding from DOE Grant DE-FG02-05ER15745 (D.G.N.) and NSF Grant CHE-0111202 (E.V.R.-A.). J.D.S. acknowledges post-doctoral NIH support (Grant GM69244). We thank Dr. David R. Manke for assistance with X-ray crystallography.

Supporting Information Available: Synthesis, characterization, and kinetic studies of Hangman salophens. This material is available free of charge via the Internet at <http://pubs.acs.org>.

IC0602087